Routes to chaos in an otpically injected semiconductor laser

Bernd Krauskopf [a], Sebastian Wieczorek [b] and Daan Lenstra [b]

[a]Dept of Engineering Mathematics, University of Bristol, Bristol BS8 1TR, UK
[b]Department of Physics and Astronomy, Vrije Universiteit Amsterdam, De Boelelaan 1081, 1081 HV Amsterdam, The Netherlands

ABSTRACT

Chaotic dynamics have been found in a single mode semiconductor laser subject to optical injection experimentally or by numerical simulation. In this paper we study this laser system by means of rate equations, which mathematically are a three-dimensional vector field. To study different routes to chaos we start from the knowledge of bifurcation curves in the plane of injection strength and detuning in Ref. [1] of this issue. Our main tool is combining the continuation of bifurcation curves with computing the respective phase space objects. In this way, we obtain detailed knowledge of regions in parameter space of different types of chaos, and what transitions can be found at the boundaries of such regions. This gives new insight into chaotic output found in experiments. Furthermore, it allows relatively easy access to chaotic dynamics for applications such as chaotic data encryption schemes.

Keywords: (semiconductor) laser, optical injection, routes to chaos, bifurcation diagram

1. INTRODUCTION

Optical injection produces an enormous variety of phenomena, especially in semiconductor lasers; see the introduction in Ref. [1] and Ref. [2] for more details. In particular, different kinds of chaotic output have been observed experimentally and in numerical simulations[3–8]. As complex nonlinear dynamics are of increasing interest for cryptography[9] and computing[10], the question arises to locate and study different types of chaos in a systematic way. This is of particular importance because it is often very difficult to distinguish in experiments between chaotic output and other complicated but nonchaotic output, or indeed between different kinds of chaotic output.

In this paper we perform a bifurcation study of the original *three-dimensional* single-mode rate equation model[1,2,11]

$$\begin{aligned} \dot{E} &= K + \left(\frac{1}{2}(1+i\alpha)n - i\omega\right) E \\ \dot{n} &= -2\Gamma n - (1+2Bn)(|E|^2 - 1) \ . \end{aligned} \tag{1}$$

Here E is the complex electric field, n is the population inversion, K is the injected field strength, and ω the detuning of the injected field from the solitary laser frequency. Furthermore, α is the linewidth enhancement factor, B is the cavity life time, and Γ is the damping rate. The parameters K and ω are important because they are the main parameters in experiments. This is why we present our results as bifurcation diagrams in the (K,ω)-plane[1,2]. Note that α, B and Γ describe material properties of the laser, and they are set to the fixed values of $\alpha = 2$, $B = 0.015$ and $\Gamma = 0.035$ throughout this paper. Equations (1) are known to show excellent agreement with experimental results[7].

Our goal is to identify different types of chaos in Eqs. (1). To this end, we take the point of view of bifurcation theory and find and continue bifurcation curves with the package AUTO[12]. In this way, regions of complicated dynamics can be identified, for which we then show the respective phase portraits obtained with the program DsTool[13]. This is quite different from computing bifurcation diagrams by numerical simulation by plotting a single parameter versus a phase space variable. In fact, our approach allows us to map out routes to chaos in unprecedented detail.

Further author information (Email addresses) –
B.K.: B.Krauskopf@bristol.ac.uk
S.M.W.: sebek@nat.vu.nl
D.L.: lenstra@nat.vu.nl

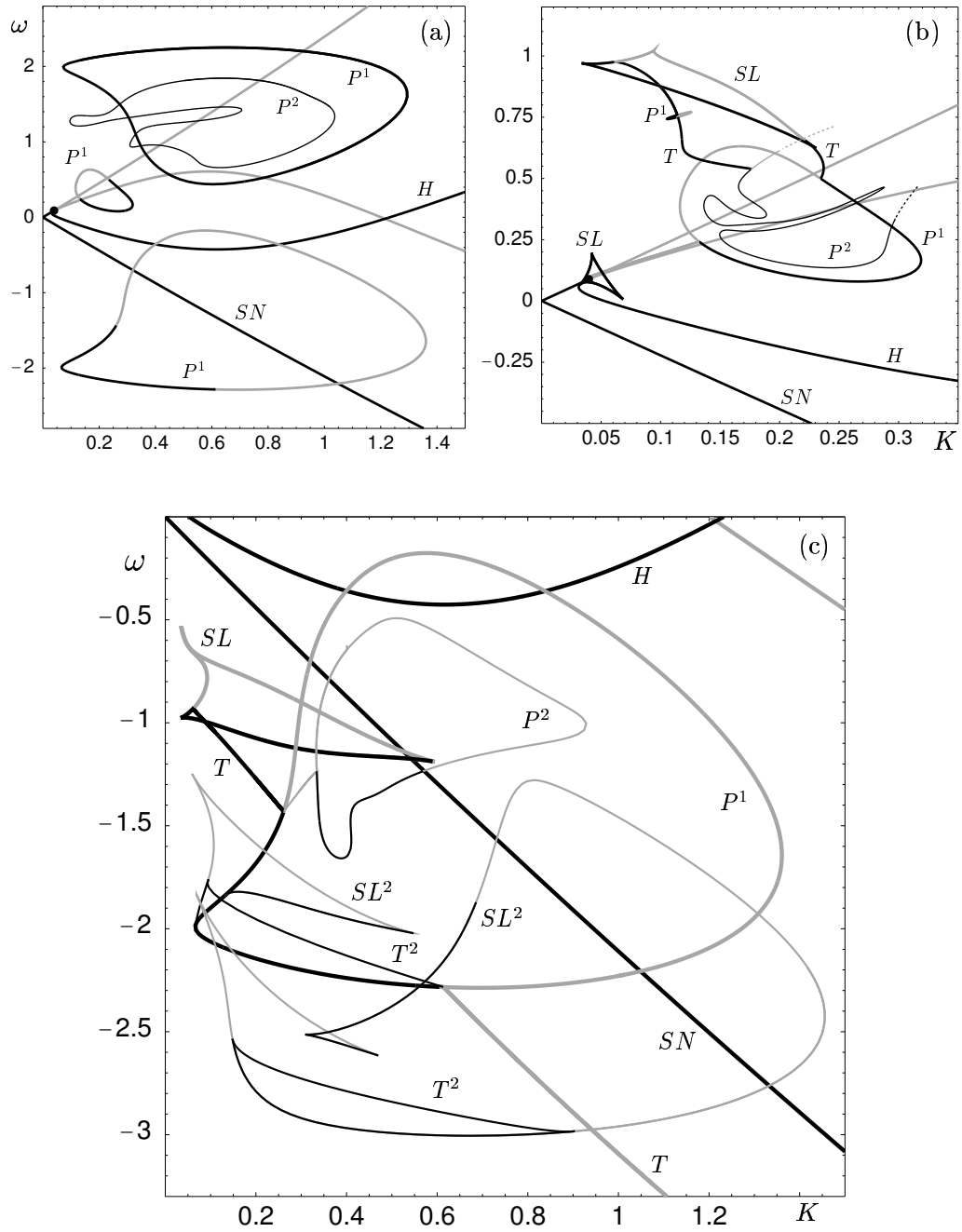

Fig. 1. Bifurcation diagrams of Eqs. (1) for $\alpha = 2$ in three different windows of the (K, ω)-plane; compare Ref. [1] for details.

Our starting point is Fig. 1 (repeated here for convenience from the respective panels in Figs. 2–4 in Ref. [1]) showing bifurcation curves of Eqns. (1) for $\alpha = 2$ in different windows of the (K, ω)-plane. Presented are saddle-node and Hopf bifurcations, period-doubling bifurcations, saddle-node of limit cycle bifurcations, and torus bifurcations. Supercritical bifurcations, in which attractors are involved, are in black, and subcritical bifurcations, in which no attractors are involved,are in grey. Superscripts in the labeling distinguish between bifurcation curves of periodic orbits of basic period and those that have already undergone a period-doubling.

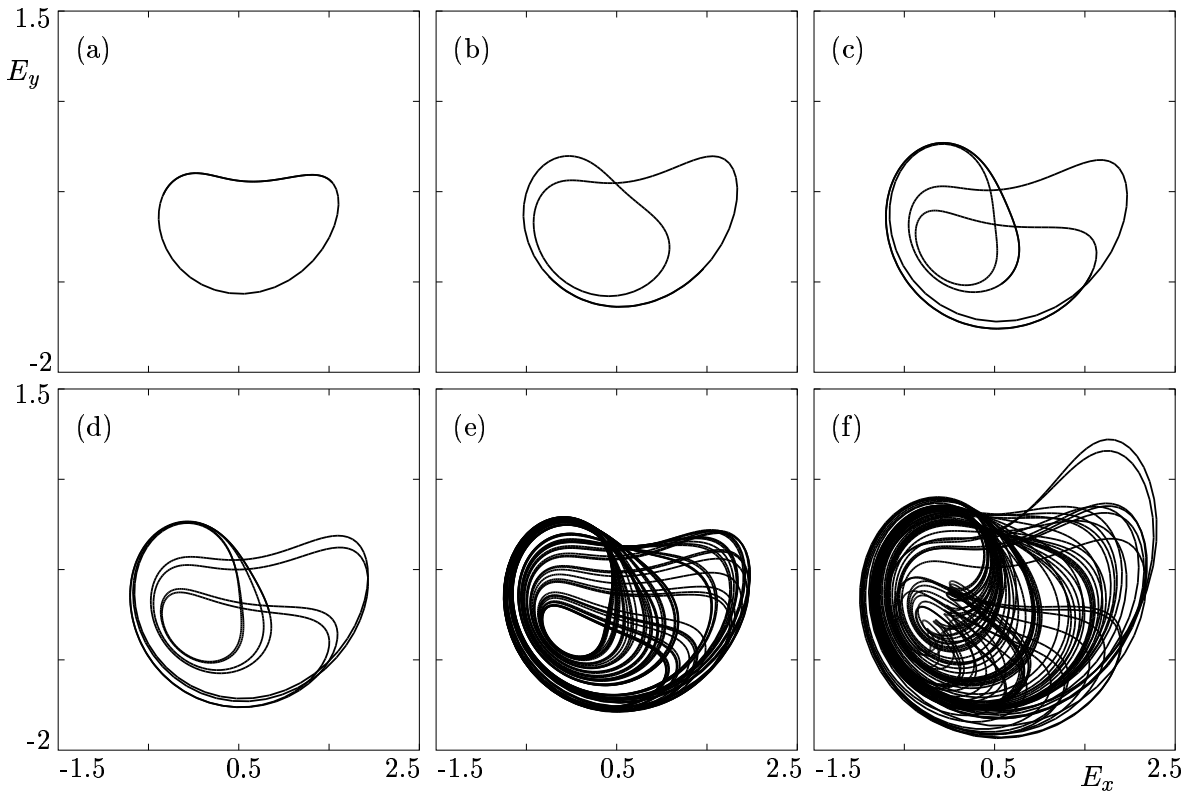

Fig. 2. Period-doubling route to chaos for $\alpha = 2$ and $K = 0.62$. Shown are projections of three-dimensional attractors onto the complex E-plane. From (a) to (f) ω takes the values 0.3, 0.5, 0.7, 0.71, 0.78, and 1.1.

The panels of Fig. 1 show an intruiging array of bifurcation curves in the (K, ω)-plane. To keep this exposition simple we concentrate here on the case $\alpha = 2$, but similar transitions can also be found for different values of α; see Ref. [1] for details. Note that not all bifurcation curves are drawn in these figures in order to keep them managable. Nevertheless, it is apparent that the bifurcation curves form a complicated structure, and are essentially all connected to each other. The curves are organized by what are called codimension-two bifurcations, which are intersection points of bifurcation curves. Typically, at these points bifurcation curves change from supercritical (black) to subcritical (grey). This highlights the necessity to follow also branches of subcritical bifurcations in order to obtain a complete and consistent bifurcation diagram in the (K, ω)-plane.

The paper is organized as follows. In Section 2 we discuss transition to chaos via period-doublings and the break-up of tori. We draw conclusions in Section 4.

2. ROUTES TO CHAOS

What happens to the dynamics as parameters are changed is best understood by presenting transitions along certain paths in the (K, ω)-plane. We present several routes to chaos, including period-doubling to chaos and the break up of tori. For typical points along such a path we then present attractors in phase space. Together with the bifurcation diagrams in Fig. 1 this gives a very detailed impression of routes to different kinds of chaotic dynamics.

2.1. Period-doubling to chaos

The nested islands of period-doubling curves in Fig. 1 (a) and (b) already hint at the presence of the period-doubling route to chaos. To illustrate this transition we take a vertical cross section through the nested islands of period-doublings in Fig. 1 (a) at $K = 0.62$. Figure 2 shows a series of three-dimensional phase portraits of Eqns. (1), projected onto the complex E-plane, along this path. An attracting periodic orbit (a) undergoes a sequence of period-doublings (b)-(d) until it apparently becomes chaotic (e) and (f).

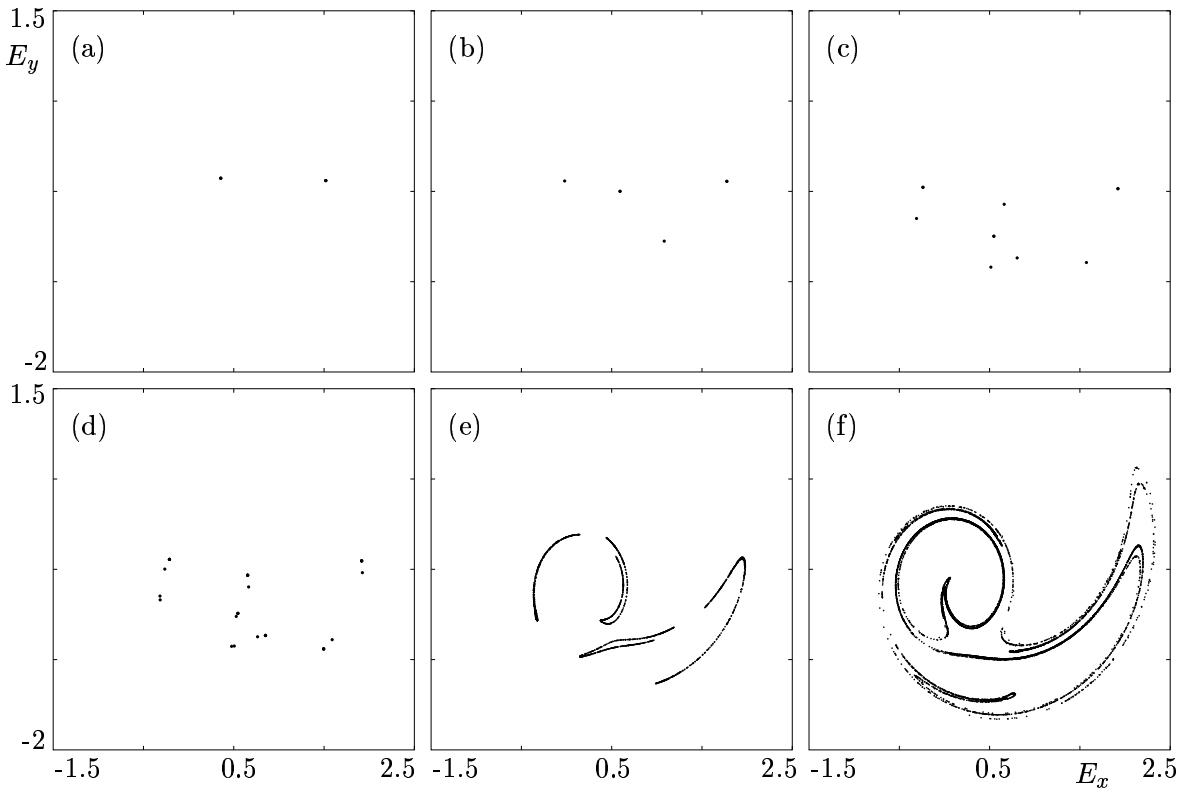

Fig. 3. The period doubling route to chaos for $\alpha = 2$ and $K = 0.62$; compare Fig. 2. Shown are attractors in the complex E-plane of the Poincaré map of the section {n=-0.1}. From (a) to (f) ω takes the values 0.3, 0.5, 0.7, 0.71, 0.78, and 1.1.

It should be noted, however, that it is very difficult to decide whether panel (e) shows a periodic orbit of high period or a choatic attractor. This is why we show in Fig. 3 the respective intersections of the attractors in Fig. 2 with the suitable section $\{n = 0.1\}$. In other words, we show the attractors of the Poincaré return map associated with this section. The period-doubling route is clearly visible in panels (a)-(d). It emerges from Fig. 3 (e) that the attractor is indeed already chaotic. It shows the typical almost one-dimensional shape of an attractor that appears after successive period-doublings. The attractor then grows further (f) into a shape that is not immediately recognizable as an attractor coming from a transition via period-doublings.

2.2. Torus break-up

In a torus bifurcation an attracting or repelling torus is born from an attracting or repelling periodic orbit. The dynamics on this torus can be locked, which means that there is an attracting orbit on this torus, or quasiperiodic, in which case trajectories fill the torus densely. Quasiperiodicity and tori were found in optically injected semiconductor lasers[14–17]. The regions where the motion on the torus is locked are called resonance tongues[18]. It is known that they are bounded by saddle-node of limit cycle bifurcations, which 'grow out of' the torus bifurcation curve at points where the so-called rotation number on the torus is rational. In Fig. 1 we show several torus curves, but not the (infinitely) many saddle-node of limit cycle bifurcations forming the resonance tongues. That these resonance tongues are present will be clear from the figures below. Here we are mainly interested in the break-up of tori and in the ensuing chaotic dynamics. This happens when a torus is followed into a region where resonance tongues start to overlap. This transition to chaos is rather spectacular, and it results in a 'much larger' chaotic attractor as can be found immediately after an accumulation of period-doublings; compare Fig. 4 (b) with Figs. 2 (e) and 3 (e).

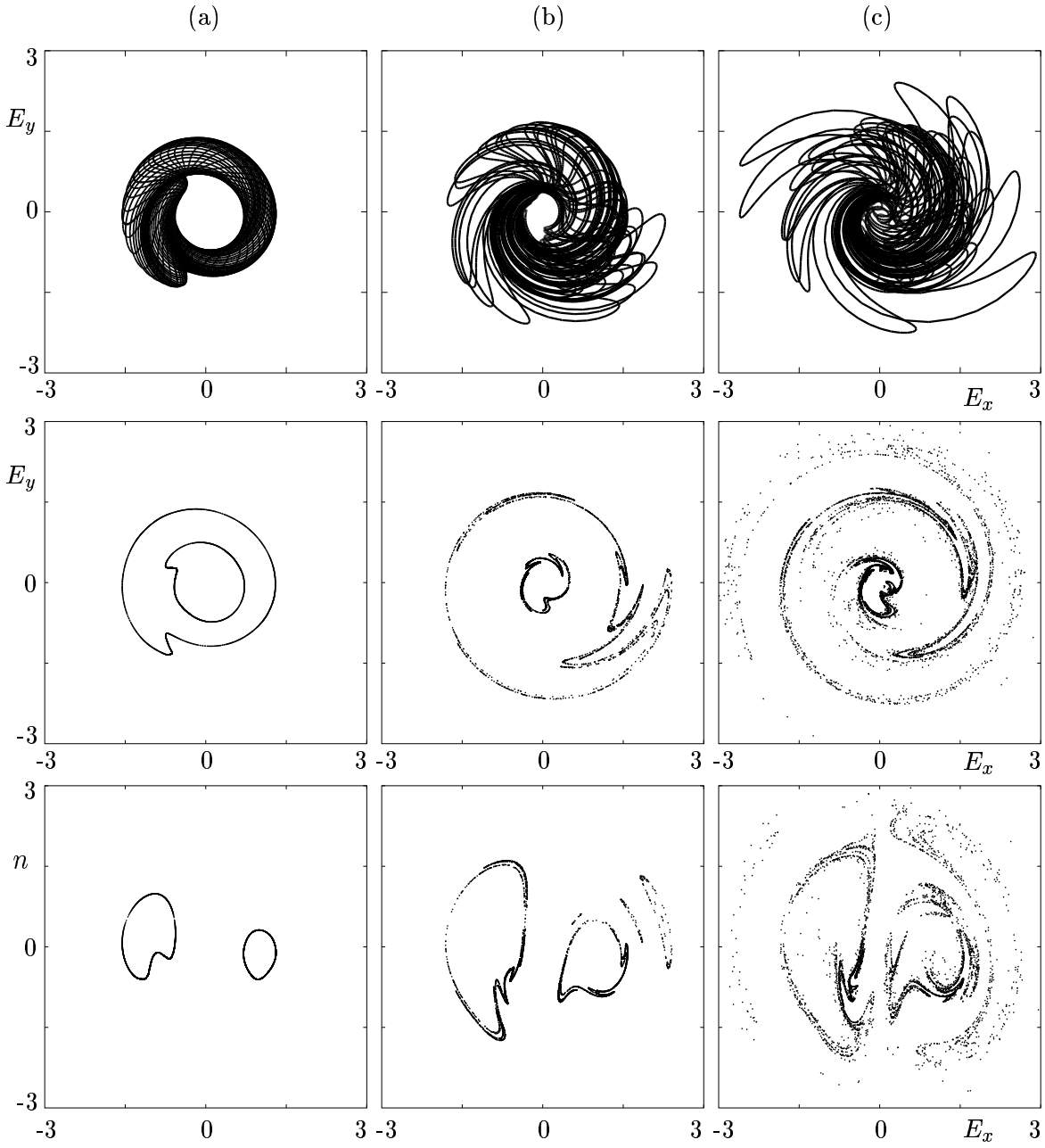

Fig. 4. Break-up of an attracting torus for $\alpha = 2$. Shown are projections of three-dimensional attractors onto the complex E-plane (top row), attractors in the complex E-plane of the Poincaré map of the section $\{n = 0\}$ (middle row), and attractors in the (E_x, n)-plane of the Poincaré map of the section $\{E_y = 0\}$ (bottom row). From left to right the parameter values are $(K, \omega) = (0.124, 0.7)$, $(K, \omega) = (0.152, 0.7)$, and $(K, \omega) = (0.179, 0.6)$.

We find an example of this transition by choosing a path through the torus curve T in Fig. 1. A representative set of phase portraits is shown in Fig. 4. Note that the first row of this figure shows three-dimensional attractors projected onto the E-plane, while the second and third rows show the attractors of the Poincaré maps associated to the sections $\{E_y = 0\}$ and $\{n = 0\}$, respecively. In this way, we get complete information about this route to chaos. The smooth torus in (a) start to lose its smoothness by forming self-similar protrusions. The attractor in (b) is already chaotic as is evidenced by its fractal structure, even though a ghost of the shape of the original torus is

still present. When the parameter is changed further the attractor becomes bigger and does not resemble the original torus any longer. We remark that the break-up of a torus goes along with complicated global bifurcations, such as homoclinic and heteroclinic bifurcations, which are present in the region of overlapping resonance tongues. We do not show all bifurcations along the route to chaos, but the phase portraits in Fig. 4 are sufficient to illustrate nicely what is happening to the torus.

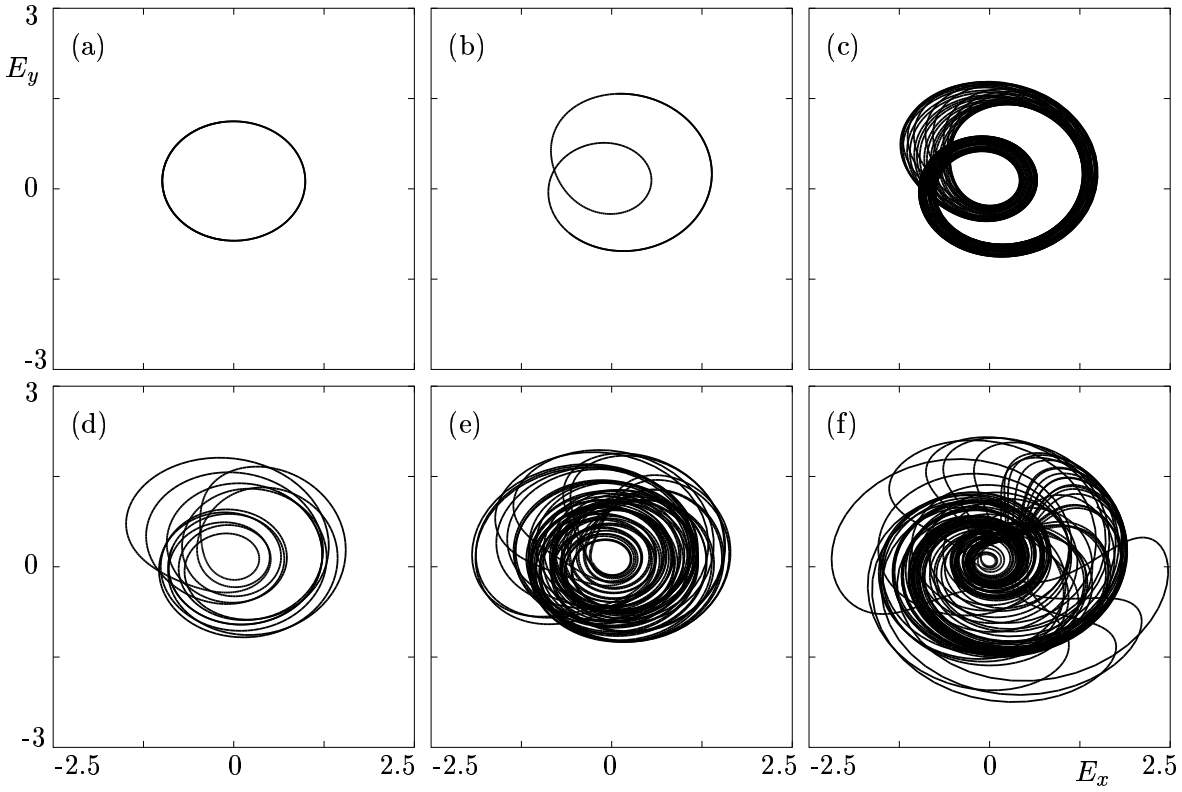

Fig. 5. Break-up of period-two torus for $\alpha = 2$ and $K = 0.23$. Shown are projections of three-dimensional attractors onto the complex E-plane. From (a) to (f) ω takes the values -2.2, -2, -1.975, -1.96, -1.93, and -1.85.

2.3. Break-up of a period-two torus

We finish by showing that the two transitions to chaos we have just discussed can occur in a mixed way: after a number of period-doublings one encounters a torus bifurcation, and the bifurcating torus of some higher base period then breaks up. This showcases the intricate interplay between bifurcation curves in Fig. 1. We demonstrate this by choosing a vertical path through Fig. 1 (c) for $K = 0.23$, which is illustrated with phase portraits in Fig. 5. The limit cyles in (a) period-doubles (b) and then undergoes a supercritical torus bifurcation when the curve T^2 in Fig. 1 (c) is crossed. This results in the emergence of a smooth attracting torus (c) that surround the origin twice in projection onto the E-plane. As ω is increased further a number of resonance tongues is crossed. An example of a locked orbit on the torus can be seen in panel (d). The torus then break up (e) and (f), which appears in a region of overlapping resonance tongues.

In order to bring out the nature of this transition to chaos we again show in Fig. 6 the corresponding attractors of a suitable Poincaré map, namely that for the section $\{E_y = 0.2\}$. The period-doubling (a) and (b) and the torus bifurcation (c) are brought out very clearly. The locked solution (d) is apparently of period 6 on the torus, which means that a respective resonance tongue was entered. It is clearly visible that the attractor in (e) is already fully chaotic, something that is hard to see in Fig. 5 (e). It has much the same structure as the attractor in Fig. 4 (b). The chaotic attractor then grows further, but does not change its overall structure very much. Interestingly, the chaotic attractors in (e) and (f) do not immediately suggest that they are born from a period-two torus. This indicates that there is substantial self interaction between the two loops of the torus.

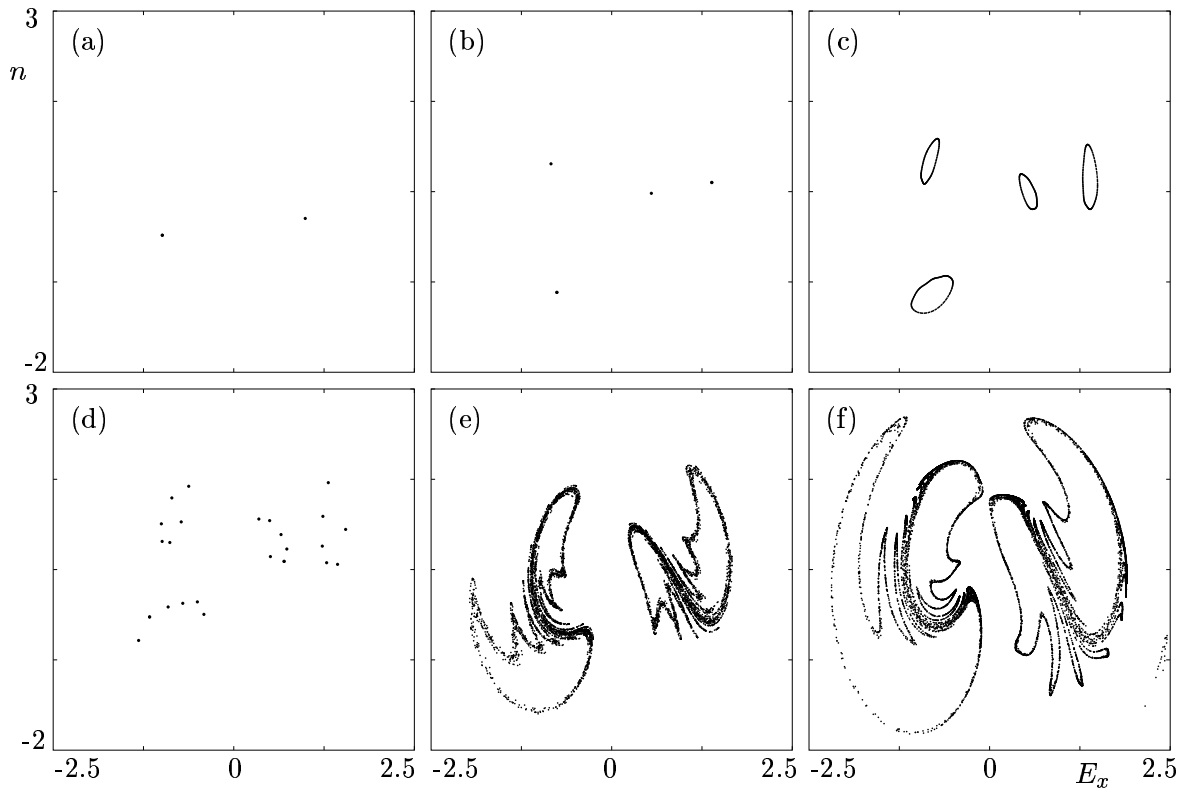

Fig. 6. Break-up of period-two torus for $\alpha = 2$ and $K = 0.23$; compare Fig. 5. Shown are attractors in the (E_x, n)-plane of the Poincaré map of the section $\{E_y = 0.2\}$. From (a) to (f) ω takes the values -2.2, -2, -1.975, -1.96, -1.93, and -1.85.

4. CONCLUSIONS

We have shown different routes to chaos in the full three-dimensional rate equations of a semiconductor laser suject to optical injection, namely that via a sequence of period-doubling, the break-up of a torus and a 'mixed transition' via the break-up of a period-two torus.

This was achieved by combining the continuation of bifurcation curves with displaying carefully selected pahse portraits of trajectories in phase space and of attractors of suitable Poincaré maps. With this technique it is possible to locate regions of different types of chaos and the possible different routes to chaos much more accurately than is possible with mere simulation. Our results are in good agreement with experimentally obtained bifurcation diagrams, and also hint at new transitions to chaos that have not been explored thotoughly by experiment.

The importance of this work lies in providing clear information of where certain types of chaotic dynamics can be found in a laser system that is experimentally quite accessible. This may allow to systematically exploit the kinds of dynamics explored here in situations where chaotic signals are needed, such as in chaotic communication schemes.

We did not perform a detailed study of homoclinic bifurcations in the systems, in particular, those responsible for the break-up of tori. It is known from bifurcation theory that there is a complicated interplay of global bifurcations in overlapping resonance tongues, and the study of this structure in a laser system remains an interesting challenge for future research.

ACKNOWLEDGEMENTS

The research of S.M.W. was supported by the Foundation for Fundamental Research on Matter (FOM), which is financially supported by the Netherlands Organization for Scientific Research (NWO).

REFERENCES

1. S.M. Wieczorek, B. Krauskopf, and D. Lenstra, "Global view of complicated dynamics in optically injected semiconductor lasers" this volume: *Proceedings SPIE* **3944** (2000).
2. S.M. Wieczorek, B. Krauskopf and D. Lenstra, "A unifying view of bifurcations in a semiconductor laser subject to optical injection", *Optics Communications* **172**(1-6) (1999) 279-295.
3. L.A. Lugiato, L.M. Narducci, D.K. Bandy, C.A. Pennise, "Breathing, spiking and chaos in a laser with injected signal", *Opt. Comm.* **46** (1983) 64–68.
4. J.R. Tredicce, F.T. Arecchi, G.L. Lippi, and G.P. Puccioni, "Instabilities in lasers with an injected signal", *J. Opt. Soc. Am. B* **2** (1) (1985) 173–183.
5. T. Erneux, V. Kovanis, A. Gavrielides, and P.M. Alsing, "Mechanism for period-doubling bifurcation in a semiconductor laser subject to optical injection", *Phys. Rev. A* **53** (6) (1996) 4372–4380.
6. V. Annovazzi-Lodi, S. Donati, and M. Manna, "Chaos and locking in a semiconductor laser due to external injection", *IEEE J. Quantum Electron.* **30** (7) (1994) 1537–1541.
7. T.B. Simpson, J.M. Liu, K.F. Huang, and K. Tai, "Nonlinear dynamics induced by external optical injection in semiconductor lasers", *Quant. Semiclass. Opt.* **9** (5) (1997) 765–784.
8. A. Gavrielides, V. Kovanis, P.M. Varangis, T. Erneux, and G. Lythe, "Coexisting periodic attractors in injection-locked diode lasers" *Quant. Semiclass. Opt.* **9** (5) (1997) 785–796.
9. C.R. Mirasso, P. Colet, and P. Garcia-Fernández, "Synchronization of chaotic semiconductor lasers: application to encoded communications", *IEEE Photonics Technology Letters* **8** (2) (1996) 299–301.
10. S. Sinha, W.L. Ditto, "Dynamics based computation", *Phys. Rev. Lett.* **81** (10) (1998) 2156–2159.
11. G.H.M. van Tartwijk, D. Lenstra, *Semiconductor lasers with optical injection and feedback*, Quant. Semiclass. Opt. **7**, 87 (1995).
12. E. Doedel, T. Fairgrieve, B. Sandstede, A. Champneys, Yu. Kuznetsov, and X. Wang, "AUTO 97: Continuation and bifurcation software for ordinary differential equations", *http://indy.cs.concordia.ca/auto/main.html*
13. A. Back, J. Guckenheimer, M.R. Myers, F.J. Wicklin, and P.A. Worfolk, "DsTool: Computer assisted exploration of dynamical systems", *Notices Amer. Math. Soc.* **39** (1992) 303-309.
14. H.G. Solari, G.L. Oppo, "Laser with injected signal: perturbation of an invariant circle", *Opt. Comm.* **111** (1994) 173–190.
15. B. Krauskopf, N. Tollenaar, and D. Lenstra, "Tori and their bifurcations in an optically injected semiconductor laser", *Opt. Comm.* **156** (1998) 158–169.
16. V. Kovanis, T.Erneux, and A. Gavrielides, "Largely detuned injection-locked semiconductor lasers", *Opt. Comm.* **159** (1999) 177–183.
17. M. Nizette, T.Erneux, A. Gavrielides, and V. Kovanis, "Injection locked semiconductor laser dynamics from large to small detunings", *Proceedings SPIE* **3625** (1999) 679-689.
18. Yu.A. Kuznetsov, *Elements of Applied Bifurcation Theory*, Applied Mathematical Sciences **112**, Springer 1995.